European Radiology (2019) 29:3111–3121
https://doi.org/10.1007/s00330-018-5898-9

HEPATOBILIARY-PANCREAS

A proposal of imaging classification of intrahepatic mass-forming cholangiocarcinoma into ductal and parenchymal types: clinicopathologic significance

Hyungjin Rhee[1] · Myeong-Jin Kim[1] · Young Nyun Park[2,3] · Chansik An[1]

Received: 6 June 2018 / Revised: 23 October 2018 / Accepted: 19 November 2018 / Published online: 17 December 2018

Abstract

Objectives To investigate the clinicopathologic significance of a subclassification of mass-forming intrahepatic cholangiocarcinoma (MF-iCCA) into ductal and parenchymal types based on magnetic resonance imaging (MRI)

Methods We enrolled 72 consecutive patients, in whom MF-iCCA was diagnosed on preoperative MRI and surgical resection from January 2000 to March 2013. Two readers independently evaluated MRI findings of adjacent bile duct dilation, periductal tumor spread, and presence of diffuse dilatation or abnormality of the intrahepatic bile duct. MF-iCCAs with none of the aforementioned findings were defined as parenchymal type, and those with one or more findings were defined as ductal type. The enhancement pattern in the arterial phase was also evaluated. Clinical and histopathological findings, as well as post-surgical outcomes, were collected from medical records.

Results Parenchymal-type MF-iCCA (21/78, 27%) exhibited significantly lower serum carbohydrate antigen 19-9 (12.8 vs. 173.8 U/mL) and carcinoembryonic antigen (1.7 vs. 4.2 ng/mL), more frequent viral hepatitis (43% vs. 18%), less frequent biliary intraepithelial neoplasia (0% vs. 26%), and less frequent perineural invasion (0% vs. 59%) and lymph node metastasis (7% vs. 46%), compared with the ductal type (57/78, 73%) ($p < 0.05$ for all). Parenchymal-type MF-iCCA showed more frequent arterial hypervascularity ($p = 0.001$) and better overall survival ($p = 0.030$) than the ductal type.

Conclusion Subclassification of MF-iCCAs into parenchymal and ductal types may be useful to discriminate clinical and histopathological characteristics and post-surgical outcomes.

Key Points

- *We propose subclassification of mass-forming intrahepatic cholangiocarcinoma (MF-iCCA) as parenchymal and ductal types, on the basis of magnetic resonance imaging findings of biliary abnormality.*
- *Two types of MF-iCCAs exhibit different clinical and histopathological characteristics and post-surgical outcomes.*

Keywords Magnetic resonance imaging · Bile ducts · Prognosis · Liver neoplasms · Bile duct diseases

✉ Myeong-Jin Kim
kimnex@yuhs.ac

[1] Department of Radiology, Research Institute of Radiological Science, Severance Hospital, Yonsei University College of Medicine, 50-1 Yonsei-Ro, Seodaemun-gu, Seoul 03722, South Korea

[2] Department of Pathology, Brain Korea 21 PLUS Project for Medical Science, Integrated Genomic Research Center for Metabolic Regulation, Yonsei University College of Medicine, Seoul, South Korea

[3] Severance Biomedical Science Institute, Yonsei University College of Medicine, Seoul, South Korea

Abbreviations

Anti-HCV	Anti-hepatitis C virus
BilIN	Biliary intraepithelial neoplasia
CA19-9	Carbohydrate antigen 19-9
CEA	Carcinoembryonic antigen
HBsAg	Surface antigen of the hepatitis B virus
iCCA	Intrahepatic cholangiocarcinoma
IQR	Interquartile range
MF-iCCA	Mass-forming intrahepatic cholangiocarcinoma
MRI	Magnetic resonance imaging
PI-iCCA	Periductal infiltrating iCCA

Introduction

Intrahepatic cholangiocarcinoma (iCCA) is an intrahepatic malignancy with biliary epithelial differentiation, arising from any part of the intrahepatic bile duct, including segmental branches to the smallest bile ducts and ductules. Increasing evidence suggests that iCCA is a heterogeneous group of tumors with varying etiologies, anatomic locations of origin, gross morphologies, histopathologies, and molecular features [1–4].

To describe the heterogeneity of iCCAs, various histologic classifications have been proposed [3, 5, 6]. According to these histological classifications, iCCA can be classified into small-duct and large-duct types. Small-duct iCCAs originating from small bile ducts or ductules are associated with chronic liver diseases, including viral hepatitis, growth without known precursor lesions, and progression to a mass-forming-type intrahepatic cholangiocarcinoma (MF-iCCA) [5]. In contrast, large-duct-type iCCAs are associated with chronic bile duct disease, including an intrahepatic stone or parasitic infection, are believed to arise from precursor lesions including biliary intraepithelial lesions or intraductal papillary neoplasms of the bile duct; and progress to periductal infiltrating or mixed periductal and mass-forming types of tumors [3].

The gross appearance of iCCA is thought to reflect the origin and progression of the tumor [3, 7]. However, dividing iCCA into three gross types, which include periductal infiltrating, intraductal growth, and mass-forming types, may not suffice in addressing the current concept of iCCA heterogeneity. Periductal infiltrating- and intraductal-type iCCAs are thought to be originated from the large bile duct, whereas MF-iCCAs are considered to be a heterogeneous group that might be originated from either the small or large bile duct. In this regard, when describing the gross appearance of an iCCA on MRI, subclassification of the MF-iCCA would be necessary.

We assumed that MF-iCCAs originated from the large bile duct would frequently show gross duct-related abnormalities, such as adjacent ductal dilatation or infiltration. We also postulated that MF-iCCAs with diffuse intrahepatic bile duct dilatation or intrahepatic stone also originated from the large bile duct, considering that underlying bile duct disease is a predisposing factor for iCCAs with large bile duct origin. Based on these findings, we introduced a new imaging classification of MF-iCCA on magnetic resonance imaging (MRI) into ductal and parenchymal types. In this subclassification, ductal-type MF-iCCA was defined as iCCAs with at least one of the aforementioned bile duct-related abnormalities, and parenchymal-type MF-iCCA was defined as those without. Therefore, the purpose of this study was to investigate the clinicopathologic significance of a subclassification of MF-iCCAs into ductal and parenchymal types based on MRI.

Methods

Patients

This retrospective study was approved by the Institutional Review Board of Severance Hospital, and the requirement for informed consent was waived. We enrolled consecutive MF-iCCA patients who had undergone surgical resection with a curative aim from January 2000 to March 2013 at Severance Hospital, Yonsei University College of Medicine (Fig. 1). We included pathologically confirmed intrahepatic cholangiocarcinoma, and determined the location of the tumor by pathologic examination of the surgical specimen. All lesions are peripheral to the second confluence of the bile duct, and tumors involving the first-order bile duct or common hepatic duct were considered perihilar cholangiocarcinoma and excluded from the present study. The primary liver carcinomas with both hepatocytic and cholangiocytic differentiation (combined hepatocellular-cholangiocarcinoma) were also excluded. The following cases were also excluded: (1) cases pretreated with any kind of preoperative treatment ($n = 12$), (2) cases without contrast-enhanced MRI within 3 months before surgery ($n = 69$), and (3) periductal infiltrating iCCAs (PI-iCCAs) ($n = 6$) or intraductal iCCAs confined to the intraductal space ($n = 16$) without demonstrable mass formation adjacent to liver parenchyma on MRI. Finally, 72 MF-iCCAs in 72 patients were included in this study (Fig. 1).

Magnetic resonance imaging

MRI was performed by using either a 1.5-T (Intera Achieva, Philips Healthcare, or Signa Horizon, GE Healthcare) or a 3.0-T (TrioTim, Siemens Healthineers, or Intera Achieva, Philips Healthcare) system with phased-array coils. The baseline MRI examination included a T2-weighted sequence and contrast-enhanced dynamic T1-weighted sequences. Pulse sequence parameters are listed in detail in Table 1. Since the subjects were recruited from an extended period of time, various contrast media were used for contrast-enhanced dynamic MR images; gadopentetate dimeglumine (Magnevist, Bayer), gadodiamide (Omniscan, GE Healthcare), gadoterate meglumine (Dotarem, Guerbet), gadobenate dimeglumine (MultiHance, Bracco Diagnostics, Inc.), or gadoxetic acid (Primovist, Bayer) was injected at 1 or 2 mL/s of 0.025 mmol/kg (for gadoxetic acid) or 0.1 mmol/kg (for contrast media other than gadoxetic acid), immediately followed by a 10- to 20-mL saline flush. Chemically selective fat-suppressed spoiled 3D gradient-recalled echo MR images were obtained during a suspended respiration of 15–25 s. Arterial phase timing was determined by using a bolus tracking or a test-bolus technique, and the scan was mostly started at 30 to 35 s (arterial phase). The second and third dynamic phases were obtained consecutively after allowing the patients

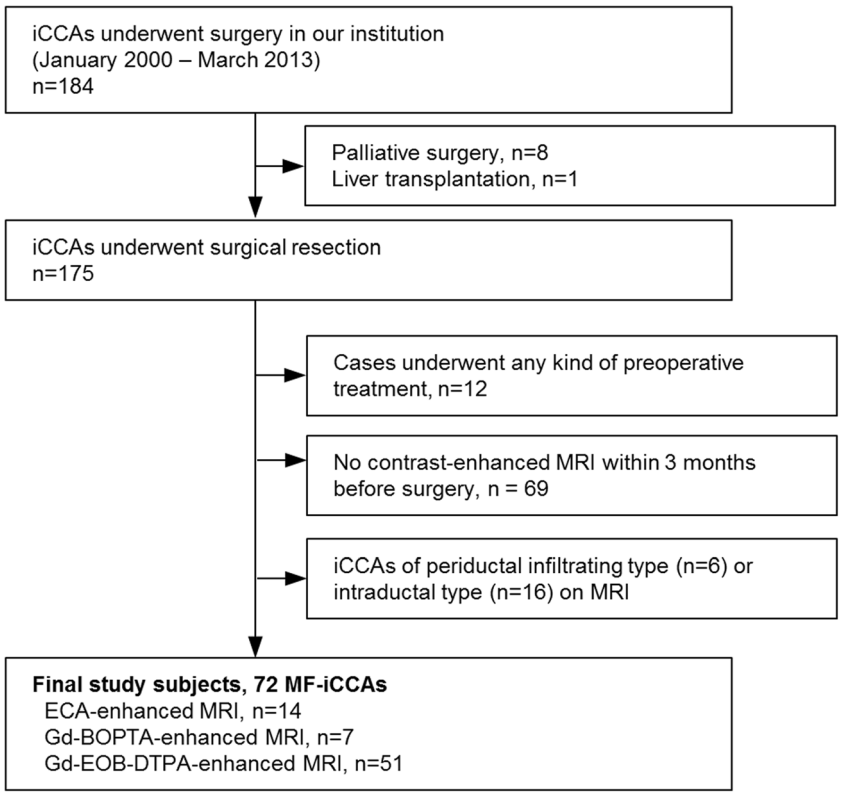

Fig. 1 Flow chart of patient inclusion and exclusion. Abbreviations: iCCA, intrahepatic cholangiocarcinoma; MRI, magnetic resonance imaging; ECA, extracellular agent; MF-iCCA, mass-forming intrahepatic cholangiocarcinoma

to have several phases of breathing following the prior scans. Equilibrium or transitional phase images were obtained approximately at 150–180 s after the injection of the intravenous contrast agent. All images were obtained in the transverse plane with a rectangular field of view of 22–24 × 38 cm, which was adjusted for each patient.

Image analysis

Two abdominal radiologists (M.J.K. and H.R.), who have 25 years and 5 years of experience in liver MRI, independently reviewed the preoperative MRI in the Picture Archiving Communication System (Centricity, GE Healthcare). The two observers were aware that the lesion was MF-iCCA, but were blinded to further clinical information and other pathologic features. The two observers categorized the MF-iCCAs into parenchymal type (Fig. 2) or ductal type (Figs. 3 and 4). Ductal-type MF-iCCAs were defined as those with at least one of the following three features: (1) adjacent bile duct dilation, obvious dilation of the bile duct adjacent to the iCCA on T2-weighted images; (2) periductal tumor spread, infiltrative soft-tissue lesion along the adjacent bile duct in a venous-phase image or T2-weighted images; or (3) presence of chronic biliary disease on T2-weighted images, such as intrahepatic stone disease or unequivocal diffuse biliary dilatation to the liver periphery suggestive of clonorchiasis. Other MF-iCCAs that were associated with none of the above three features were defined as parenchymal type.

Table 1 Summary of the protocol of pulse sequences of magnetic resonance imaging

	T2-weighted image				T1-weighted dynamic image			
Field strength (vendor)	1.5 T (GE)	1.5 T (Philips)	3.0 T (Philips)	3.0 T (Siemens)	1.5 T (GE)	1.5 T (Philips)	3.0 T (Philips)	3.0 T (Siemens)
Matrix	256–288 × 230–256	256 × 256	288 × 232	256 × 192	256 × 160	320 × 224	256 × 258	256 × 192
Section thickness, mm	7–8	7	5	6	8–10	3	4	2
Intersection gap, mm	2–5	5	1	1	0	0	0	0
Repetition time, ms	2000–10,900	452	1314	2000	180–200	3.9	3.0	2.54
Echo time, ms	80–190	80–160	80	88	1.5–2.2	1.1	1.4	0.95
Flip angle, °	90	90	90	150	90	25	10	13

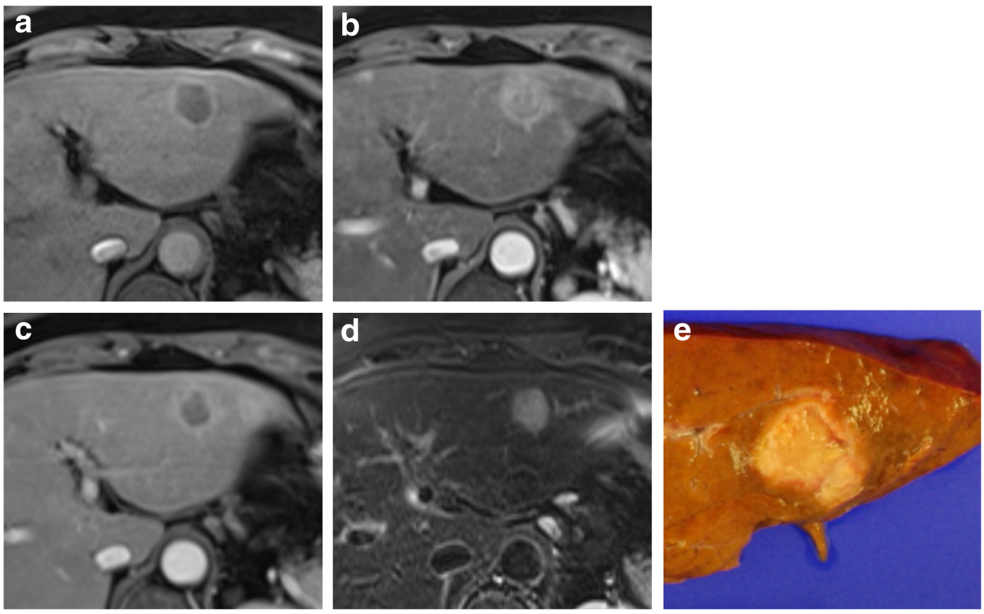

Fig. 2 A 51-year-old female with parenchymal-type mass-forming intrahepatic cholangiocarcinoma (MF-iCCA). A patient with hepatitis C virus-related chronic hepatitis. A 2.0-cm MF-iCCA exhibited low-signal intensity in precontrast T1-weighted imaging (**a**), global hyperenhancement in the arterial phase (**b**), and washout on the early portal phase (**c**) of gadoxetic acid-enhanced magnetic resonance imaging. There was no dilation or tumor infiltration along the adjacent bile ducts in T2-weighted images (**d**) and on gross specimen analysis (**e**)

Arterial enhancement patterns were also analyzed as follows: (1) hypovascular pattern, no identifiable hyperenhancing portion relative to surrounding liver parenchyma; (2) thin-rim pattern, rim-like enhancement of non-measurable thickness; (3) partially hypervascular pattern, thick rim-like enhancement with measurable thickness or heterogeneous enhancement in < 50% of the tumor area; and (4) globally hypervascular pattern, hyperenhancement in > 50% of the tumor area. Two weeks after completing the initial review, the two radiologists met together to establish by consensus the final opinion for parenchymal/ductal types and arterial enhancement patterns in cases on which they had first disagreed.

Clinical and histopathologic data

Clinical and histopathologic data including age, sex, serum tumor markers and viral markers, surgical pathological results, and post-surgical outcome were retrospectively collected from the electronic medical record and pathology reports of our institution. The pathologic T stage followed the seventh

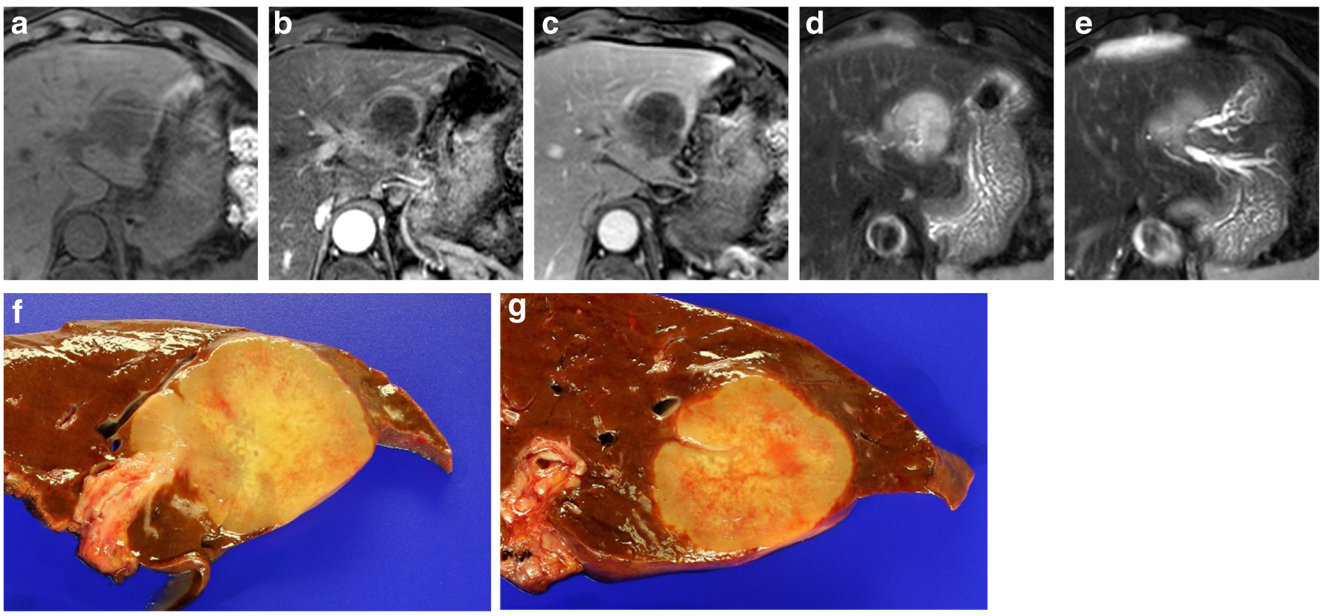

Fig. 3 A 63-year-old male with ductal-type mass-forming intrahepatic cholangiocarcinoma (MF-iCCA). A 5-cm MF-iCCA in the left lateral segment showed low signal intensity in precontrast T1-weighted images (**a**), thin-rim arterial enhancement pattern (**b**), hypointensity in the early portal phase (**c**), and moderate signal intensity of the tumor and adjacent bile duct dilation in T2-weighted images (**d** and **e**). On gross specimen analysis (**f** and **g**), bile duct involvement of the tumor was not shown

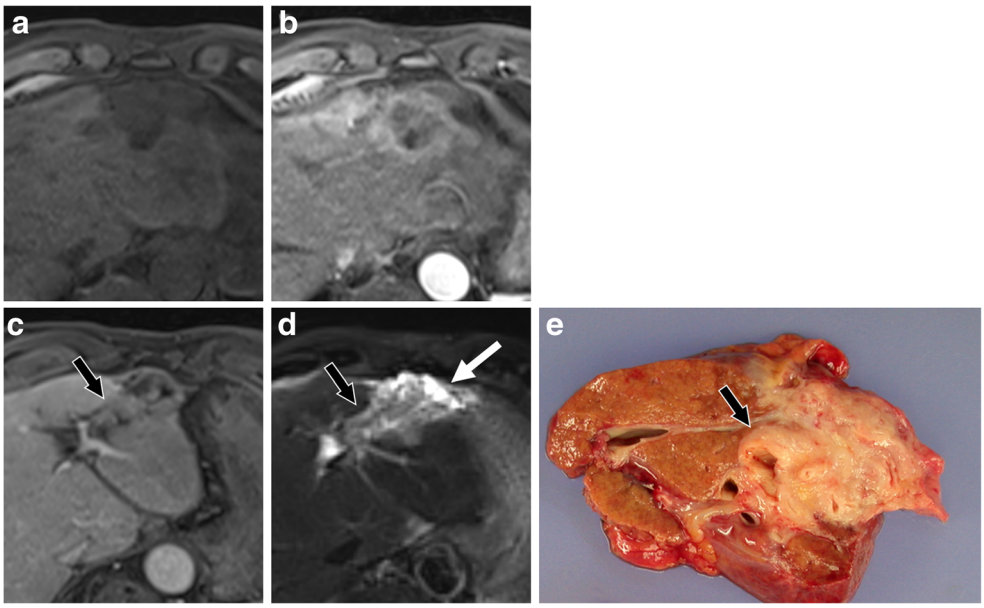

Fig. 4 A 59-year-old male with ductal-type mass-forming intrahepatic cholangiocarcinoma (MF-iCCA). The MF-iCCA in segment 3 shows hypointensity on precontrast T1-weighted imaging (**a**), thin-rim pattern on the arterial phase (**b**), and periductal tumor spread along the adjacent segmental bile duct (black arrow) on the portal phase (**c**) of gadoxetic acid-enhanced magnetic resonance imaging. The periductal tumor spread (black arrow), and distal bile duct dilatation along the subcapsular area (white arrow) is also noted on T2-weighted images (**d**).The gross specimen (**e**) also shows periductal tumor spread (black arrow)

edition of the American Joint Cancer Committee staging for iCCA. The pathologic gross type was recorded in accordance with the description on the original pathologic reports [8]. After hepatic resection, the patients were routinely followed up using computed tomography (or MRI) with serum marker (carbohydrate antigen 19-9 [CA19-9] and/or carcinoembryonic antigen [CEA]) at intervals of 3 to 6 months. The post-surgical outcome of all patients was checked in January 2017. The endpoints were defined as follows: overall survival was defined as the time between surgical resection and death of any cause, and disease-free survival was defined as the time between surgical resection and radiological or pathological evidence of the first tumor recurrence. Patients who were lost to follow-up were censored at the point of the last follow-up. We compared the 5-year overall survival and disease-free survival rates between ductal- and parenchymal-type MF-iCCAs.

Statistical analysis

Inter-reader agreement was expressed by Cohen's kappa coefficient. A kappa statistic of 0.8–1.0 was considered excellent agreement, 0.6–0.79 good agreement, 0.40–0.59 moderate agreement, 0.2–0.39 fair agreement, and 0–0.19 poor agreement. To compare clinical and histopathologic features, we used the Mann-Whitney *U* test for continuous variables and the chi-square or Fisher's exact test for categorical variables. Pairwise deletion was used for management of missing data. Two-sided p values < 0.05 were considered statistically significant. All statistical analyses were performed with SPSS software (version 23.0, SPSS Inc.).

Results

Baseline characteristics of MF-iCCAs

The median age of the patients was 63 years (interquartile range [IQR], 55–70 years), and 39 (54%) of the patients were male (Table 2). Twenty-two (31%) patients had chronic hepatitis or liver cirrhosis, and 18 patients (25%) were positive for serum surface antigen of the hepatitis B virus (HBsAg) or anti-hepatitis C virus (HCV). Five (7%) patients had hepatolithiasis, and 13 (18%) showed biliary intraepithelial neoplasia (BilIN) on pathologic examination. The median size of the MF-iCCAs was 4.4 cm (IQR, 3.1–6.0 cm). On pathologic examination, the majority of MF-iCCAs ($n = 58$, 81%) were reported as mass-forming type, but the remaining three (4%) and 11 (15%) were reported as PI type and mixed MF and PI type, respectively. The median follow-up duration was 37 months (IQR, 13–62 months).

Distinct clinical and pathologic characteristics between parenchymal-type and ductal-type MF-iCCAs

Of the 72 MF-iCCAs, 21 (29%) were classified as parenchymal type and 51 (71%) as ductal type by reviewer 1. By reviewer 2, 17 (24%) were classified as parenchymal type and 55 (76%) as ductal type. The interobserver agreement for the imaging classification was good, with a kappa coefficient of 0.644. The reviewers' opinions were different in 10 of 72 cases (14%). In detail, the reviewers' opinions were different for ① adjacent duct dilatation in six cases, ② periductal tumor spread in three cases, and ③ presence of diffuse ductal dilatation or abnormality in one case. Opinions differed

Table 2 Comparison of clinicopathological features between parenchymal-type and ductal-type intrahepatic mass-forming cholangiocarcinomas (MF-iCCA)

Clinicopathologic features	Total ($n = 72$, 100%)	Parenchymal-type MF-iCCA ($n = 21$, 29%)	Ductal-type MF-iCCA ($n = 51$, 71%)	p value[a]
Age (years), median (IQR)	63 (55–70)	61 (51–68)	64 (56–70)	0.143
Sex, male/female (%)	39 (54%)/33 (46%)	11 (52%)/10 (48%)	28 (55%)/23 (45%)	1.000
Serum markers				
CA19-9 (U/mL), median (IQR)[b]	51.8 (7.9–404.3)	12.8 (3.4–29.8)	173.8 (13.4–1660.5)	0.004
CEA (ng/mL), median (IQR)[b]	2.5 (1.5–7.4)	1.7 (1.1–2.1)	4.3 (1.6–11.8)	0.010
AFP (IU/mL), median (IQR)[b]	2.2 (1.7–4.6)	3.1 (1.8–5.3)	2.2 (1.7–3.6)	0.337
PIVKA-II (mAU/mL), median (IQR)[b]	23.0 (18.0–29.0)	24.0 (18.5–33.3)	22.0 (17.8–29.0)	0.544
HBsAg(+) and/or anti-HCV(+) (%)	18 (25%)	9 (43%)	9 (18%)	0.036
Non-tumoral pathology				
Chronic hepatitis or cirrhosis (%)	22 (31%)	10 (48%)	12 (24%)	0.054
Hepatolithiasis (%)	5 (7%)	1 (5%)	4 (8%)	1.000
Biliary intraepithelial neoplasia (%)	13 (18%)	0 (0%)	13 (26%)	0.008
Tumoral pathology				
Tumor size (cm), median (IQR)	4.4 (3.1–6.0)	3.5 (2.3–4.6)	5.0 (3.5–6.5)	0.025
Gross morphology on pathologic exam				0.124
Mass forming	58 (81%)	20 (95%)	38 (75%)	
Mixed mass forming and periductal infiltrating	11 (15%)	1 (5%)	10 (20%)	
Periductal infiltrating	3 (4%)	0 (0%)	3 (6%)	
Differentiation				0.064
Well differentiated	17 (25%)	8 (38%)	9 (18%)	
Moderately differentiated	42 (58%)	8 (38%)	34 (67%)	
Poorly differentiated	12 (17%)	4 (19%)	8 (16%)	
Undifferentiated	1 (1%)	1 (5%)	0 (0%)	
Microvascular invasion (%)	55 (76%)	18 (86%)	37 (73%)	0.361
Tumor multiplicity (%)	8 (11%)	1 (5%)	7 (15%)	0.423
Perineural invasion (%)[b]	30 (42%)	0 (0%)	30 (59%)	< 0.001
Lymph node metastasis (%)[b]	21 (36%)	1 (7%)	20 (46%)	0.011
pT stage (T1/T2/T3/T4) (%)	16 (22%)/36 (50%)/16 (22%)/4 (6%)	6 (29%)/15 (71%)/0 (0%)/0 (0%)	10 (20%)/21 (41%)/16 (31%)/4 (8%)	0.009
Imaging finding				
Arterial enhancement pattern (hypo/thin-rim/partially hypervascular/globally hypervascular)	18 (25%)/27 (38%)/18 (25%)/9 (13%)	2 (10%)/5 (24%)/7 (33%)/7 (33%)	16 (31%)/22 (43%)/11 (22%)/2 (4%)	0.001

Abbreviations: *IQR* interquartile range, *CA19-9* carbohydrate antigen 19-9, *CEA* carcinoembryonic antigen, *AFP* alpha-fetoprotein, *PIVKA-II* protein induced by vitamin K absence/antagonist-II

[a] p values were calculated by chi-square, Fisher's exact test, or Mann-Whitney U test

[b] Serum CA19-9, CEA, AFP, PIVKA-II, perineural invasion, and lymph node metastasis have missing values in 4, 12, 22, 34, 1, and 14 cases, respectively

between reviewers when the duct dilatation was not severe or the degree of infiltration was weak. In consensus review, the cases were classified as ductal type when adjacent ductal involvement was apparent even if the degrees of ductal dilatation or infiltration were weak. Finally, by consensus, 21 (29%) were classified as parenchymal type and 51 (71%) as ductal type (Table 2). The numbers of cases showing each combination of the ductal-type MRI findings were as follows: ① + ② + ③, $n = 0$ (0%); ① + ②, $n = 8$ (11%); ① + ③, $n = 14$ (19%); ② + ③, $n = 1$ (1%); ① only, $n = 23$ (32%); ② only, $n = 4$ (6%);③ only, $n = 1$ (1%); and none in parenchymal type ($n = 21$, 29%).

The parenchymal-type MF-iCCAs exhibited significantly lower levels of serum CA19-9 and CEA ($p = 0.004$ and $p = 0.010$, respectively), and were more frequently associated with positivity in serum viral markers ($p = 0.036$) than the ductal-type MF-iCCAs. On pathologic examination, the ductal-type MF-iCCAs were associated with the presence of

BilIN ($p = 0.008$). Most ($n = 20$, 95%) of the parenchymal-type MF-iCCAs were reported on pathologic reports as MF type and one (5%) as mixed MF and PI type, whereas a considerable proportion of ductal-type MF-iCCAs were reported as mixed type ($n = 10$, 20%) or PI type ($n = 3$, 6%). The ductal-type MF-iCCAs showed a larger tumor size ($p = 0.025$), frequent perineural invasion and lymph node metastasis ($p < 0.001$ and $p = 0.011$, respectively), and advanced pathologic T-stage ($p = 0.009$), compared with the parenchymal type. As the parenchymal/ductal types were associated with tumor size, we additionally performed the subgroup analysis by the tumor size (Table 3). We divided MF-iCCAs by tumor size of 4.4 cm, which corresponds to the median size of this cohort, and compared characteristics of parenchymal and ductal types (Table 3). In both size ranges, parenchymal and ductal types exhibited similar trends of clinicopathologic characteristics. Among all tumors that were smaller than 4.4 cm, the ductal type was associated with higher serum CA19-9 ($p = 0.017$) and frequent perineural invasion ($p < 0.001$). Among tumors that were equal to or larger than 4.4 cm, ductal-type tumors were associated with higher serum CEA ($p = 0.017$), poorer differentiation ($p = 0.039$), and frequent perineural invasion ($p = 0.045$).

Comparison of arterial enhancement patterns between parenchymal-type and ductal-type MF-iCCAs

Of the 72 MF-iCCAs, by consensus, nine (13%), 18 (25%), 27 (38%), and 18 (25%) were classified as globally hypervascular, partially hypervascular, thin-rim, and hypovascular MF-iCCAs, respectively (Table 2). The interobserver agreement for arterial enhancement pattern was excellent, with a kappa coefficient of 0.827. Parenchymal-type MF-iCCAs frequently showed arterial hypervascularity; approximately 33% ($n = 7$) and 33% ($n = 7$) of parenchymal-type MF-iCCAs exhibited globally and partially hypervascular patterns, respectively. In contrast, ductal-type MF-iCCAs frequently demonstrated hypovascular (31%, $n = 16$) and thin-rim (43%, $n = 22$) patterns on arterial-phase images ($p = 0.001$) (Fig. 5a).

Differences in post-surgical outcome of MF-iCCAs between parenchymal-type and ductal-type MF-iCCAs

Parenchymal type MF-iCCAs showed better 5-year overall survival, compared with ductal-type MF-iCCAs (59% vs. 32%, $p = 0.030$) (Fig. 5b). However, disease-free survival was not significantly different between parenchymal- and ductal-type MF-iCCAs ($p = 0.437$) (Fig. 5c). We also performed subgroup analysis of overall survival by tumor size (Fig. 5d). In MF-iCCAs smaller than 3.1 cm (25 percentile of tumor size) and equal to or larger than 6.0 cm (75 percentile of tumor size), overall survival is statistically not significant. In MF-iCCAs between 3.1 and 6.0 cm, overall survival of the parenchymal type was significantly better than that of the ductal type ($p = 0.017$).

Discussion

The iCCAs are a group of heterogeneous tumors, in which histopathologic findings, etiologies, anatomical locations of origin, gross appearance, molecular profiles, and clinical outcomes have been shown to be associated with each other [1, 5, 9–17]. Microscopic findings are generally difficult to visualize in cross-sectional imaging; therefore, gross findings that reflect the heterogeneity of iCCA, such as the location and gross morphology, might be considered for imaging descriptions of iCCA heterogeneity. Aishima et al reported that iCCAs originating from either a second branch or a segmental branch often histologically resemble large bile duct epithelium, and therefore are considered as large duct type; on the other hand, iCCAs originating from a smaller duct than a segmental branch often resemble small duct epithelium, and is considered as small duct type [5]. However, anatomical locations of iCCAs are frequently difficult to specify if the tumor is large (> 5 cm); in addition, even if the tumor is small, the tumor arising in the small bile duct could involve the adjacent large bile duct [10, 11]. Therefore, instead of anatomical location, the gross appearance of iCCA might be appropriate for describing the heterogeneity of iCCA.

Based on MRI findings of the coexistence of biliary abnormalities, we subclassified MF-iCCAs into parenchymal- or ductal-type MF-iCCAs. Our results showed that parenchymal-type MF-iCCAs were associated with chronic liver disease, and most (95%) were MF-iCCA on gross pathologic classification. Ductal-type MF-iCCAs were associated with BilIN and with high serum tumor markers, including CA19-9 and CEA. Ductal-type MF-iCCAs also exhibited a larger tumor size, frequent perineural invasion and lymph node metastasis, higher pathologic T-stage, and poor overall survival after surgical resection. Histopathologic small-duct-type MF-iCCAs are reported to be associated with chronic liver disease or cirrhosis and MF morphology, whereas large-duct-type MF-iCCAs are associated with BilIN, perineural invasion, and lymph node metastasis [11, 12, 14, 17]. Therefore, parenchymal-type and ductal-type MF-iCCAs have histologic characteristics of MF-iCCAs of small duct and large duct origins, respectively.

It is worth noting that perineural invasion and lymph node metastasis are rarely observed in parenchymal-type MF-iCCAs (0% and 7%, respectively), whereas they are frequently observed in ductal-type MF-iCCAs (59% and 46%, respectively). Perineural invasion and lymph node metastasis are well-known poor prognostic factors that are only assessable in surgical specimens, and are reported to be frequent in the histologic large-duct-type MF-iCCA

Table 3 Comparison of clinicopathological features between parenchymal-type and ductal-type intrahepatic mass-forming cholangiocarcinomas (MF-iCCA), subgroup analysis by the tumor size

Clinicopathologic features	Tumor size < 4.4 cm ($n = 36$)			Tumor size ≥ 4.4 cm ($n = 36$)		
	Parenchymal-type iCCA ($n = 16$, 44%)	Ductal-type iCCA ($n = 20$, 56%)	p value[a]	Parenchymal type iCCA ($n = 5$, 14%)	Ductal type iCCA ($n = 31$, 86%)	p value[a]
Age (years), median (IQR)	59 (50–67)	66 (55–71)	0.083	62 (58–72)	63 (57–68)	0.894
Sex, male/female (%)	10 (63%)/6 (38%)	9 (45%)/11 (55%)	0.335	1 (20%)/4 (80%)	19 (61%)/12 (39%)	0.149
Serum markers						
CA19-9 (U/mL), median (IQR)[b]	14.2 (3.3–29.8)	219.0 (16.8–409.0)	0.017	8.4 (5.1–145.0)	136.9 (7.8–5630.0)	0.162
CEA (ng/mL), median (IQR)[b]	1.8 (1.6–2.7)	2.8 (1.0–6.8)	0.307	1.3 (0.9–1.7)	4.5 (1.8–31.3)	0.011
AFP (IU/mL), median (IQR)[b]	2.7 (1.9–5.8)	2.2 (2.2–3.0)	0.799	5.2 (3.0–5.2)	2.0 (1.7–3.7)	0.742
PIVKA-II (mAU/mL), median (IQR)[b]	23.0 (19.0–38.5)	23.0 (15.0–26.0)	0.471	25.0 (17.5–26.5)	21.0 (18.0–32.0)	0.611
HBsAg(+) and/or anti-HCV(+) (%)	8 (50%)	4 (20%)	0.081	1 (20%)	5 (16%)	1.000
Non-tumoral pathology						
Chronic hepatitis or cirrhosis (%)	9 (56%)	6 (30%)	0.175	1 (20%)	6 (19%)	1.000
Hepatolithiasis (%)	0 (0%)	1 (5%)	1.000	1 (20%)	3 (10%)	0.466
Biliary intraepithelial neoplasia (%)	0 (0%)	4 (20%)	0.113	0 (0%)	9 (29%)	0.302
Tumoral pathology						
Tumor size (cm), median (IQR)	3.2 (2.2–3.8)	3.0 (2.2–3.7)	0.838	6.0 (5.0–13.0)	6.0 (5.0–7.5)	0.657
Gross morphology on pathologic exam			0.060			1.000
Mass forming	15 (94%)	12 (60%)		5 (100%)	26 (84%)	
Mixed mass forming and periductal infiltrating	1 (6%)	5 (25%)		0 (0%)	5 (16%)	
Periductal infiltrating	0 (0%)	3 (15%)		0 (0%)	0 (0%)	
Differentiation			0.156			0.039
Well differentiated	6 (38%)	3 (15%)		2 (40%)	6 (19%)	
Moderately differentiated	7 (44%)	15 (75%)		1 (20%)	19 (61%)	
Poorly differentiated	3 (19%)	2 (10%)		1 (20%)	6 (19%)	
Undifferentiated	0 (0%)	0 (0%)		1 (20%)	0 (0%)	
Microvascular invasion (%)	13 (81%)	14 (70%)	0.700	5 (100%)	23 (74%)	0.566
Tumor multiplicity (%)	1 (6%)	1 (5%)	1.000	0 (0%)	6 (19%)	0.564
Perineural invasion (%)[b]	0 (0%)	12 (60%)	< 0.001	0 (0%)	18 (58%)	0.045
Lymph node metastasis (%)[b]	1 (11%)	7 (47%)	0.178	0 (0%)	13 (45%)	0.132
pT stage (T1/T2/T3/T4) (%)	6 (38%)/10 (63%)/0 (0%)/0 (0%)	5 (25%)/9 (45%)/4 (20%)/2 (10%)	0.123	0 (0%)/5 (100%)/0 (0%)/0 (0%)	5 (16%)/12 (39%)/12 (39%)/2 (7%)	0.090
Imaging finding						
Arterial enhancement pattern (hypo/thin-rim/partially hypervascular/ globally hypervascular)	0 (0%)/3 (19%)/6 (38%)/7 (44%)	7 (35%)/6 (30%)/6 (30%)/1 (5%)	0.007	2 (40%)/2 (40%)/1 (20%)/0 (0%)	9 (29%)/16 (52%)/5 (16%)/1 (3%)	0.922

Abbreviations: *IQR* interquartile range, *CA19-9* carbohydrate antigen 19-9, *CEA* carcinoembryonic antigen, *AFP* alpha-fetoprotein, *PIVKA-II* protein induced by vitamin K absence/antagonist-II

[a] p values were calculated by chi-square, Fisher's exact test, or Mann-Whitney U test

[b] Serum CA19-9, CEA, AFP, PIVKA-II, perineural invasion, and lymph node metastasis have missing values in 4, 12, 22, 34, 1, and 14 cases, respectively

[12, 14, 15, 17–19]. The classification of ductal- and parenchymal-type MF-iCCAs might serve as a preoperative non-invasive method to estimate risk of microscopic perineural and lymph node metastasis.

Additionally, several studies have suggested that the presence of arterial enhancement is frequently observed in small-duct-type, rather than large-duct-type, MF-iCCAs and that iCCAs with arterial hypervascularity were associated with favorable outcome [11, 20–23]. In the present study, parenchymal-type MF-iCCAs were more commonly hypervascular in the arterial phase, and showed favorable overall survival compared to the ductal type.

Recently, several histopathologic classifications of small- and large-duct-type iCCAs have been proposed; however, consensus criteria have not yet been established. Although they are based on a similar concept of the histopathologic or molecular similarity to small- and large-duct epithelium, there are significant differences between them. For example, one report proposed criteria based on the anatomical location of the iCCA origin [5], while others proposed criteria based on histopathologic morphology [11, 13, 14, 17], mucin production [11, 12], or specific protein expression [12, 14]. Regarding histopathologic morphology, most recent reports have described the mixed

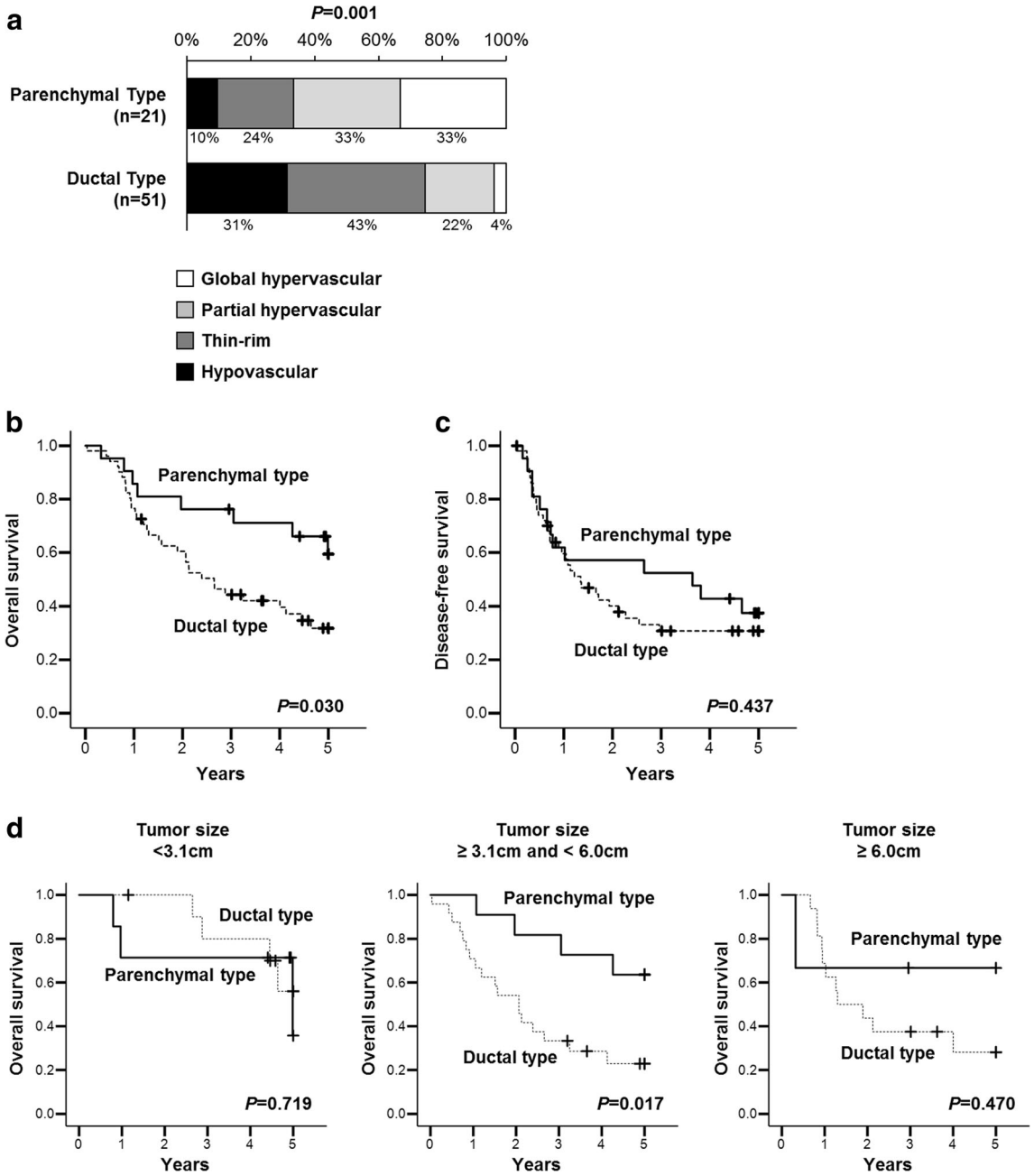

Fig. 5 Arterial phase enhancement pattern and post-surgical outcome. **a** Comparison of arterial phase enhancement patterns between parenchymal- and ductal-type mass-forming intrahepatic cholangiocarcinomas (MF-iCCAs). Kaplan-Meier plot for overall survival (**b**) and disease-free survival (**c**) of parenchymal- and ductal-type MF-iCCAs. Subgroup analysis for overall survival by 25- and 75-percentiles of tumor size (**d**)

small- and large-duct-type histology of iCCA [11, 13, 14, 17] and the way classifications differ between reports. Some reports have used the threshold percentage of the tumor area (varying from 10 to 80% for small-duct-type iCCA) [14, 17], and others have used the location of small-duct-type histology in the mixed case [13]. However, it still remains unclear which criteria would be optimal for clinical and prognostic characterization of iCCA.

The parenchymal or ductal type that we termed in the present study is a description of the gross appearance of iCCA and is not intended to predict histopathologic small or large duct types. Although our data showed that parenchymal and ductal types are strongly associated with various clinicopathologic findings of small duct type and large duct type, respectively, histologic types and our imaging types might not be exactly matched in all cases. Nevertheless, our subclassification of MF-iCCA into

parenchymal and duct related on MRI would still be valuable, as it is easy to classify, in addition to showing high interobserver agreement and providing clinically relevant clinicopathologic and prognostic information on the basis of the modern concept of iCCA heterogeneity in the preoperative stage.

Our study has several limitations. As MF-iCCA is a relatively rare primary liver cancer, our study cohort was retrospectively collected over a long period to include as many patients as possible. For this reason, the MR instruments, protocols, and contrast media are rather heterogeneous. In particular, enhancement of iCCA may differ between MRIs using hepatobiliary and extracellular contrast agents. However, our MRI classification of MF-iCCAs was primarily based on the gross appearance of the iCCA, not the specific enhancement pattern; therefore, our classification could be clinically feasible for various MRI protocols. Another limitation of our study is that our imaging classification was based on MRI and may be difficult to apply to other imaging modalities, such as computed tomography or ultrasound, due to the superior soft-tissue contrast of MRI for the visualization of duct dilation and periductal spread; therefore, MRI evaluation may be required for more accurate imaging classification.

In conclusion, we propose subdividing MF-iCCAs into parenchymal and ductal types that can be easily discerned on MRI; these show different causative factors, distinct clinical and histopathological characteristics, and divergent post-surgical outcomes.

Funding This study was supported by a grant from the National R&D Program for Cancer Control, Ministry of Health & Welfare, Korea (Grant No. 1520160).

Compliance with ethical standards

Guarantor The scientific guarantor of this publication is Myeong-Jin Kim.

Conflict of interest Myeong-Jin Kim is a recipient of a grant from Bayer HealthCare, which is not related to this study.

Statistics and biometry No complex statistical methods were necessary for this paper.

Informed consent Written informed consent was waived by the Institutional Review Board.

Ethical approval Institutional Review Board approval was obtained.

Study subjects or cohorts overlap Some study subjects or cohorts have been previously reported in Rhee et al [14].

Methodology
- Retrospective
- Observational
- Performed at one institution

References

1. Banales JM, Cardinale V, Carpino G et al (2016) Expert consensus document: cholangiocarcinoma: current knowledge and future perspectives consensus statement from the European Network for the Study of Cholangiocarcinoma (ENS-CCA). Nat Rev Gastroenterol Hepatol 13:261–280
2. Razumilava N, Gores GJ (2014) Cholangiocarcinoma. Lancet 383: 2168–2179
3. Aishima S, Oda Y (2015) Pathogenesis and classification of intrahepatic cholangiocarcinoma: different characters of perihilar large duct type versus peripheral small duct type. J Hepatobiliary Pancreat Sci 22:94–100
4. Ebata T, Ercolani G, Alvaro D, Ribero D, Di Tommaso L, Valle JW (2016) Current status on cholangiocarcinoma and gallbladder cancer. Liver Cancer 6:59–65
5. Aishima S, Kuroda Y, Nishihara Y et al (2007) Proposal of progression model for intrahepatic cholangiocarcinoma: clinicopathologic differences between hilar type and peripheral type. Am J Surg Pathol 31:1059–1067
6. Nakanuma Y, Kakuda Y (2015) Pathologic classification of cholangiocarcinoma: new concepts. Best Pract Res Clin Gastroenterol 29:277–293
7. Lim JH, Park CK (2004) Pathology of cholangiocarcinoma. Abdom Imaging 29:540–547
8. Yamasaki S (2003) Intrahepatic cholangiocarcinoma: macroscopic type and stage classification. J Hepatobiliary Pancreat Surg 10:288–291
9. Nakanuma Y, Curado MP, Franceschi S, Gores GJ, Paradis V, Sripa B, Tsui WMS, Wee A (2010) Intrahepatic cholangiocarcinoma. In: Bosman FT, Carneiro F Hruban RH, Theise ND (Eds) WHO classification of tumours of the digestive system, 4th edn. World Health Organization. pp 217–224
10. Nakanuma Y, Sato Y, Harada K, Sasaki M, Xu J, Ikeda H (2010) Pathological classification of intrahepatic cholangiocarcinoma based on a new concept. World J Hepatol 2:419–427
11. Komuta M, Govaere O, Vandecaveye V et al (2012) Histological diversity in cholangiocellular carcinoma reflects the different cholangiocyte phenotypes. Hepatology 55:1876–1888
12. Hayashi A, Misumi K, Shibahara J et al (2016) Distinct clinicopathologic and genetic features of 2 histologic subtypes of intrahepatic cholangiocarcinoma. Am J Surg Pathol 40:1021–1030
13. Akita M, Fujikura K, Ajiki T et al (2017) Dichotomy in intrahepatic cholangiocarcinomas based on histologic similarities to hilar cholangiocarcinomas. Mod Pathol 30:986–997
14. Rhee H, Ko JE, Chung T et al (2018) Transcriptomic and histopathological analysis of cholangiolocellular differentiation trait in intrahepatic cholangiocarcinoma. Liver Int 38:113–124
15. Andersen JB, Spee B, Blechacz BR et al (2012) Genomic and genetic characterization of cholangiocarcinoma identifies therapeutic targets for tyrosine kinase inhibitors. Gastroenterology 142: 1021–1031 e1015
16. Sia D, Hoshida Y, Villanueva A et al (2013) Integrative molecular analysis of intrahepatic cholangiocarcinoma reveals 2 classes that have different outcomes. Gastroenterology 144:829–840
17. Liau JY, Tsai JH, Yuan RH, Chang CN, Lee HJ, Jeng YM (2014) Morphological subclassification of intrahepatic cholangiocarcinoma: etiological, clinicopathological, and molecular features. Mod Pathol 27:1163–1173
18. Wang Y, Li J, Xia Y et al (2013) Prognostic nomogram for intrahepatic cholangiocarcinoma after partial hepatectomy. J Clin Oncol 31:1188–1195
19. Shirai K, Ebata T, Oda K et al (2008) Perineural invasion is a prognostic factor in intrahepatic cholangiocarcinoma. World J Surg 32:2395–2402

20. Nam JG, Lee JM, Joo I et al (2018) Intrahepatic mass-forming cholangiocarcinoma: relationship between computed tomography characteristics and histological subtypes. J Comput Assist Tomogr 42:340–349
21. Kim SA, Lee JM, Lee KB et al (2011) Intrahepatic mass-forming cholangiocarcinomas: enhancement patterns at multiphasic CT, with special emphasis on arterial enhancement pattern—correlation with clinicopathologic findings. Radiology 260:148–157
22. Fujita N, Asayama Y, Nishie A et al (2017) Mass-forming intrahepatic cholangiocarcinoma: enhancement patterns in the arterial phase of dynamic hepatic CT—correlation with clinicopathological findings. Eur Radiol 27:498–506
23. Yoshida Y, Imai Y, Murakami T et al (1999) Intrahepatic cholangiocarcinoma with marked hypervascularity. Abdom Imaging 24: 66–68